Original Article

JVS

Evaluation of the ureteral jet in dogs by using color Doppler ultrasonography

Hyunjung Oh[1], Seongsoo Kim[1], Suyeon Kim[1], Jeosoon Lee[1], Sookyung Yun[1], Junghee Yoon[1], Joohyun Jung[2], Mincheol Choi[1,*]

[1]Department of Veterinary Medical Imaging, College of Veterinary Medicine, Seoul National University, Seoul 08826, Korea
[2]Ilsan Animal Medical Center, Goyang 10368, Korea

Ureteral jets are the result of a forceful ejection of urine from the vesicoureteral junction into the urinary bladder. By using color Doppler ultrasonography (US), we aimed to identify distinct ureteral jets in dogs, provide insight into ureteral obstruction, and facilitate study of urodynamics and vesicoureteric sphincter function via pulsed Doppler US. Color Doppler US was applied to detect urinary flow from the right ureteral orifices in eight healthy beagles. Under anesthesia, 0.9% saline (2.5 mL/kg/h) and furosemide (0.5 mg/kg) were administered intravenously to assist in detection of distinct ureteral jets and examine their frequency, velocity, duration, and waveform. In all dogs, ureteral jets were visualized under diuresis and anesthesia within 2 to 5 min (mean 3.57 ± 0.90 min) of the furosemide injection. Mean frequency, peak velocity, and duration of right ureteral jets in seven dogs in whom six ureteral jet waveform patterns were identified were 9.86 ± 3.09 jets/min, 34.07 ± 10.02 cm/sec, and 2.82 ± 1.08 sec, respectively. During the 10 min period starting 10 min after the initial jet appeared, only three waveforms were identified. Color Doppler US of ureteral jets may aid in assessing vesicoureteric sphincter function and ureteral abnormalities, such as ureteral obstruction, in dogs.

Keywords: Doppler ultrasonography, dogs, ureteral jet, ureteral obstruction

Introduction

The term ureteral jet refers to a urinary flow in which urine is ejected forcefully from the vesicoureteral junction (VUJ) into the urinary bladder lumen via peristaltic contraction of the ureter. On two-dimensional ultrasonography (US), ejected urine is visualized in the form of a low-intensity echogenic stream from the ureteral orifice. However, color Doppler US demonstrates this phenomenon more clearly, and the use of pulsed Doppler US allows further characterization of the jet [5,10,19,20,29,30]. Many previous studies on humans have addressed several issues, such as why the jet is detected [20,30], the incidence of jet visualization and its frequency [19], the velocity and duration of the jet [5,28,29], symmetry of left and right jets [3], temporal fluctuation in jets [15], effect of hydration on the jet [41], clinical applications such as ureteric patency [4], and the pattern of the jet's Doppler waveform [5,15,24,26,41].

However, it may be more difficult to identify the ureteral jet during ultrasonographic examination in animals such as dogs because of several limitations, including the need for physical constraints on the animals, locational differences in urinary specific gravity, and degree of distention of the urinary bladder. Therefore, in veterinary medicine, the results of studies on the ureteral jet phenomenon remain inconclusive. A previous study described the clinical application of assessing the ureteral jet in dogs and suggested that non-visualization of the ureteral jet could assist in the diagnosis of ectopic ureter [23]. Despite controversy regarding the clinical utility of the ureteral jet in humans, the detection of a urine jet flow has been considered useful in the evaluation of ureteral obstruction, for which the presence of a ureteral jet can be used to exclude complete obstruction [1,8,18,31]. Previous Doppler US studies of the ureteral jet have suggested the presence of a functionally active sphincter with myogenic and neurogenic components at the human VUJ [24,25,26,32]. The existence of the ureteral jet phenomenon and its association with a VUJ valvular mechanism has been reported in dogs [7,16]. The primary purpose of this study was to describe the ureteral jet phenomenon in dogs, under general anesthesia and with diuretic administration. In addition, Doppler US was used to determine whether ureteral jets can be visualized with sufficient

consistency to aid in the evaluation of ureteral obstruction and ureter urodynamics. We hypothesized that the VUJ sphincter in dogs has an active mechanism, not simply a valve mechanism, that can be characterized by the pulsed Doppler waveform of the ureteral jet; a mechanism similar to that observed in humans.

Materials and Methods

Eight adult beagle dogs, including two females and six males (weight range, 7.8−13.5 kg; mean, 11.3 ± 1.90 kg) were included in this study. Complete blood counts; serum biochemistry profiles, including blood urea nitrogen, creatinine, and electrolyte analyses; and urinalysis revealed no abnormalities.
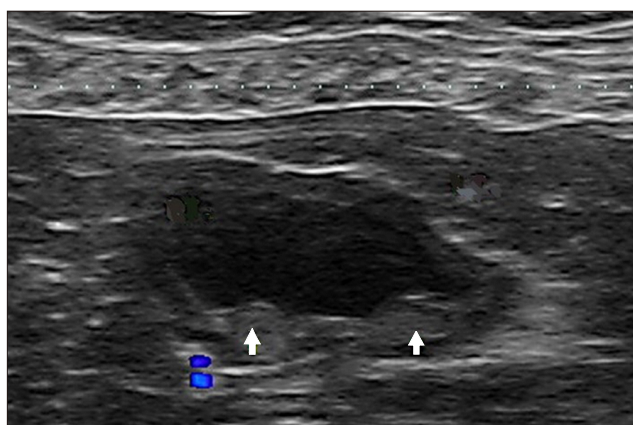
Color Doppler ultrasonographic examination was performed by using a commercially available unit (Aloka Prosound α7; Hitachi Aloka Medical, Japan) with a 4−11 MHz linear transducer. The pulse-repetition frequency was 5 kHz. Intravenous 0.9% saline was administered to each dog at a rate of 2.5 mL/kg/h to provide sufficient hydration and facilitate identification of the ureteral jet. The urinary bladder was scanned in dorsal recumbency to assess the degree of distention. Real-time examination was performed in each dog when the urinary bladder was partially distended. Anesthetic (Zoletil 50; Virbac, France) was injected intravenously at a dose of 5 mg/kg, and an equal amount of the anesthetic was injected into the antebrachial muscle region. Under anesthesia, the ureteral orifices were identified in the transverse imaging plane (Fig. 1). To obtain a clear image of the right ureteral orifice and jet, the probe was moved craniomedially, with the right orifice serving as the axis (Fig. 2). Then, 0.5 mg/kg furosemide (Lasix Injection; Handok, Korea) was injected in order to detect the

Fig. 1. Transverse ultrasonographic image of the urinary bladder showing two small elevations of the mucosal surface representing the ureteral orifices (arrows) on the dorsal aspect.
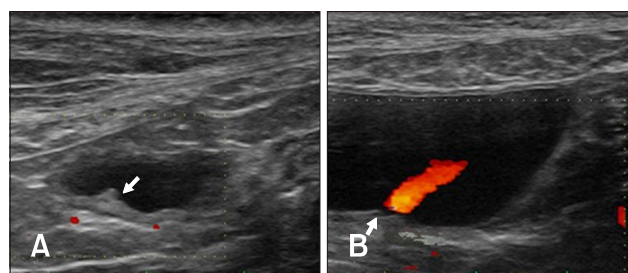

Fig. 2. Oblique ultrasonographic image of the urinary bladder clearly showing the orifice (A) and the jet flow (B). The anechoic area within the elevation represents the right ureter (arrows).
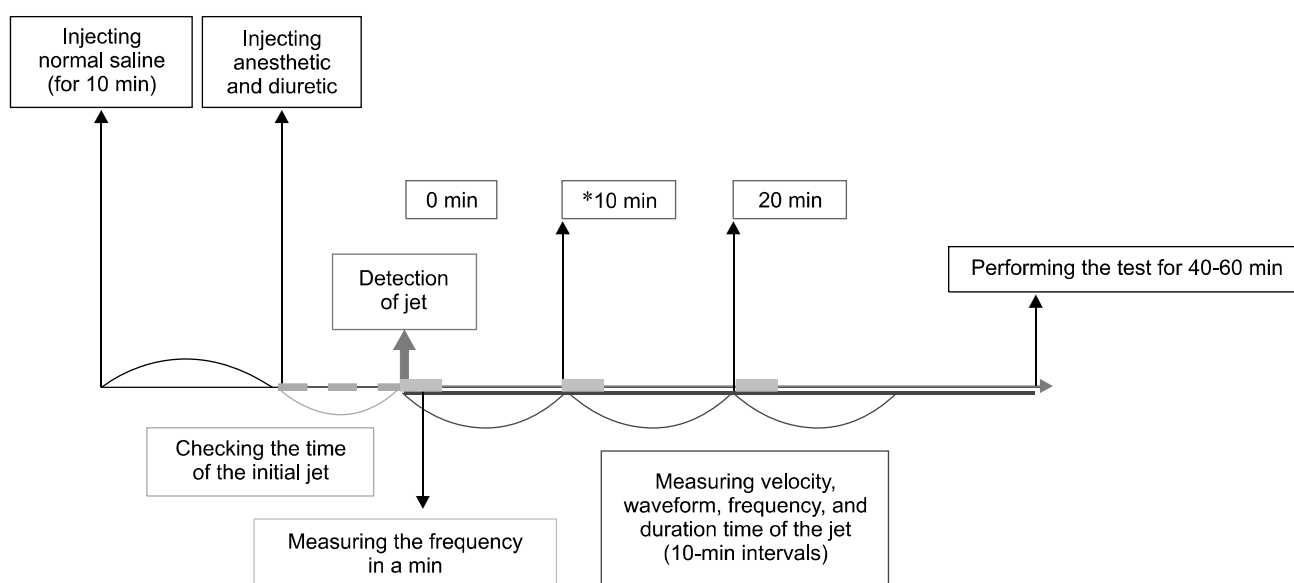

Fig. 3. Schematic diagram of the experimental procedure. *Period in which the jet is identified most distinctively.

ureteral jet from the orifice. The orifice was observed until the ureteral jet was identified. After color signals were detected, the initial time and frequency were recorded. The scan axis was rotated to the axis of the jet, and spectral waveforms were obtained as close as possible to the right orifice. Between jets, the Doppler cursor was carefully maintained directly over the ureteral orifice. Even slight displacement of the cursor from the center of the jet led to poor spectral waveforms, which were rejected. In dogs with the jet perpendicular to the dorsal surface of the bladder, scanning had to be performed from a lateral position in order to obtain a valid Doppler angle and reveal spectral waveforms.

Receiver gain and output were altered to optimize visualization. The Doppler gate was opened with sufficient width to include the entire jet, and it was centered at the point of maximum flow. The Doppler angle was set parallel to the streamline in the center of the jet and limited to within the range of 30° to 60°, as far as possible. Real-time color Doppler US and

Fig. 4. Spectral Doppler image of the right ureteral orifice. The peak velocity (c) is approximately 47.8 cm/sec, and the duration time (T) is 2.0 sec. The waveform is monophasic. a, point of commencement of the Doppler signal; b, termination of signal; V, velocity.

spectral waveforms were recorded for 40 to 60 min (Fig. 3). When a jet was not identified, the examination was terminated before 40 min had elapsed, and the urinary bladder height was measured on a transverse scan. The features of the jet flow were measured by the pulsed Doppler system, and the waveform was obtained by performing Doppler wave spectral analysis (Fig. 4). The frequency, duration time, velocity, and waveform of the ureteral jets were measured during the period in which the ureteral jets were most frequent (*i.e.*, the 10 min period beginning 10 min after detection of the initial jet) (Fig. 3). The waveform was categorized according to the human waveform system of classifying ureteral jets [24-26].

Results

Ureteral jets were detected by performing color Doppler US in all eight dogs (100%). The left and right VUJs were visible as two protuberances on the mucous layer when a probe was moved from the urethra to the bladder neck on a transverse scan (Fig. 1). At irregular intervals, a burst of color flow was observed to emanate from one or both ureteral orifices; these commonly occurred separately but occasionally occurred in concert. On oblique scan, the probe was moved craniomedially, with the right orifice serving as the axis, and the right ureteral orifice was identified clearly as a mucosal elevation. The right ureter was displayed as an anechoic area within a bulging structure on the mucosal surface (panel A in Fig. 2). The flow toward the transducer was assigned a red color (panel B in Fig. 2). The oblique scan image was chosen for optimal depiction of jets from the right side, and the depicted jet did not interfere with that from the left side.

In seven of the eight dogs, the ureteral jets were cranial or craniomedial (panel B in Fig. 2). Occasionally, they were perpendicular to the mucosal layer, similar to that observed in human studies [3,5,8,20,21]. One dog was excluded from the spectral Doppler study because the direction of its jet flow (color-coded blue) was different from those of the other dogs.
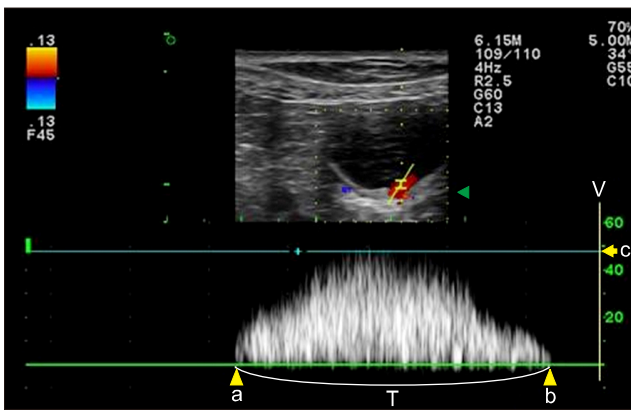
Table 1. Ureteral jet parameters detected during the 10 min period starting 10 min after the initial appearance of a ureteral jet

Dog number	Initial time (min)	Frequency (jets/min)	Average peak velocity* (cm/sec)	Average duration* (sec)	Waveform
1	5	6	20.37 ± 3.17	4.21 ± 0.67	Continuous
2	2	9	33.66 ± 3.86	2.18 ± 0.22	Square
3	3	9	55.57 ± 2.61	2.57 ± 0.08	Square
4	4	8	29.26 ± 0.64	1.81 ± 0.04	Square
5	3	8	31.56 ± 1.93	3.15 ± 0.25	Continuous
6	4	15	30.66 ± 2.98	1.37 ± 0.13	Monophasic
7	4	14	36.66 ± 2.21	4.15 ± 0.21	Continuous

*Values presented are means ± SD.

The time at which the initial jet appeared ranged from 2 to 5 min (mean, 3.57 ± 0.90 min) after the furosemide injection. The initial jet was clearly detected within 5 min in all dogs. The results for each dog are listed in Table 1, and the mean initial time is shown in Fig. 5. When the range-gated Doppler device was arranged to provide a sample volume that coincided with the area of the trigone craniomedial to the ureteral orifice, various Doppler signals were obtained (Fig. 4). The results obtained from each dog are shown in Tables 1 and 2. Six ureteral jet waveform patterns, similar to those reported in humans, were identified [24-26]. These six waveform patterns were based on the number of peaks within a single ureteral jet and are categorized as follows: monophasic (only one peak), biphasic (two peaks), triphasic (three peaks), polyphasic (four or more peaks), square (a plateau pattern with no distinct peak and within the average duration), and continuous (an irregular plateau or no peak with a duration exceeding the mean duration) (Fig. 6) [24,26]. During the period in which the ureteral jets occurred most frequently, that is, the period starting 10 min after the initial jet appeared, only three waveforms were identified. Among the seven dogs, three (42.9%), three (42.9%), and one dog (14.2%) exhibited continuous, square, and monophasic waveforms, respectively (Table 1).
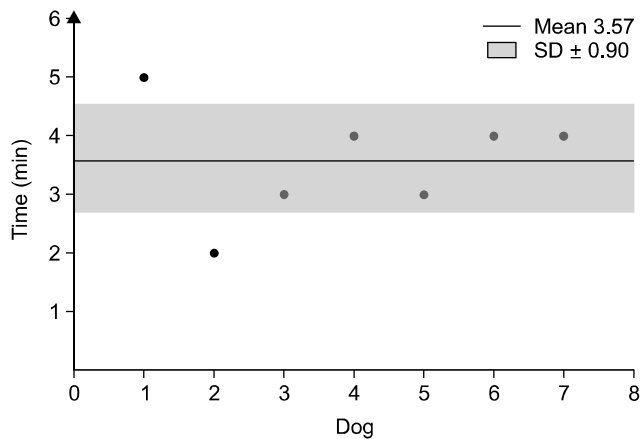

Fig. 5. The mean and standard deviation of the initial time of appearance of ureteral jets. Note that the jet phenomenon occurred in each dog (except Dog 8) within 5 min of injection of the diuretic.
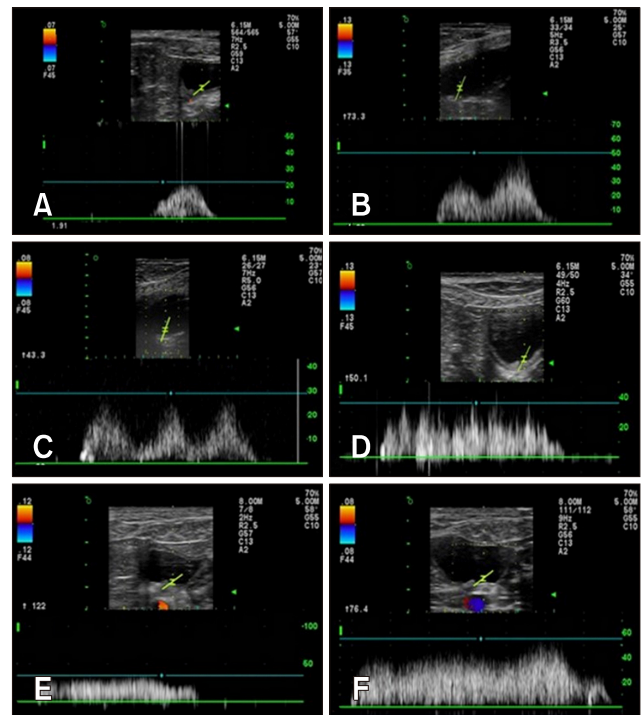

Fig. 6. Six distinctive waveform patterns of the ureteral jet. (A) Monophasic waveform. (B) Biphasic waveform. (C) Triphasic waveform. (D) Polyphasic waveform. (E) Square waveform. (F) Continuous waveform.

Table 2. Changes in parameters over time in each dog and the height of the bladder when the jet was no longer detected

Dog number	Time (min)	Frequency (jets/min)	Change in jet appearance	Bladder height (cm)	Changes in parameters (v, f, d)
1	60	4	No change in appearance	–	Reduced/f
2	60	8	Jet flow disappeared but was visualized as red dots	5.12	Reduced/v, f, d
3	30	5	Absence of a jet (at 40 min)	5.83	Reduced/f, d
4	60	8	Jet flow disappeared but was visualized as red dots	4.41	Reduced/v, d
5	50	7	Jet flow disappeared but was visualized as red dots	5.79	Reduced/v, f, d
6	50	8	No change in appearance	–	Reduced/v, f, d
7	30	10	Absence of a jet (at 40 min)	5.27	Reduced/v, f, d

v, velocity; f, frequency; d, duration.

The measured duration of individual jets varied from 1.19 to 4.86 sec. The average duration in each of the seven dogs included in the analysis ranged from 1.81 to 4.41 sec, and the mean duration in the seven dogs was 2.82 ± 1.08 sec. The results obtained from each dog are shown in Table 1, while the mean duration in each dog and the mean duration in all dogs are plotted in Fig. 7. In six of the seven dogs, the average jet duration decreased over time. In three of these six dogs, a red color-coded ureteral jet was not observed, but a red spot was identified at the orifice region. There was a complete absence of a color signal in two of the six dogs (Table 1). The Doppler waveform of the red color-coded spots was an extremely short monophasic waveform with a duration reduced to fractions of a second (panel D in Fig. 8). Only one of the seven dogs exhibited a consistent jet without any change in duration; however, the frequency of the jets decreased (Table 1). Five dogs in which either the ureteral jets disappeared or were displayed as red color-coded spots at the orifice region had notably distended bladders (Table 2).

The measured peak velocity of the individual jets varied from 15.30 to 60.60 cm/sec. The average peak velocities in the seven dogs included in the analysis ranged from 20.37 to 55.37 cm/sec, and the mean peak velocity in these dogs was 34.07 ± 10.02 cm/sec (Fig. 9). Five of the seven dogs exhibited a decrease in peak velocity over time. In four of these five dogs, the decrease in duration was usually accompanied by a reduction in peak velocity (Table 2). The frequency of jets ranged from 6 to 15 jets/min in the seven dogs included in the analysis (mean, 9.86 ± 3.09 jets/min) (Table 1). Over time, the frequency of jets declined in six of the seven dogs. All seven dogs displayed a decrease in at least one of the jet parameters (peak velocity, duration, or frequency) over time (Table 2).
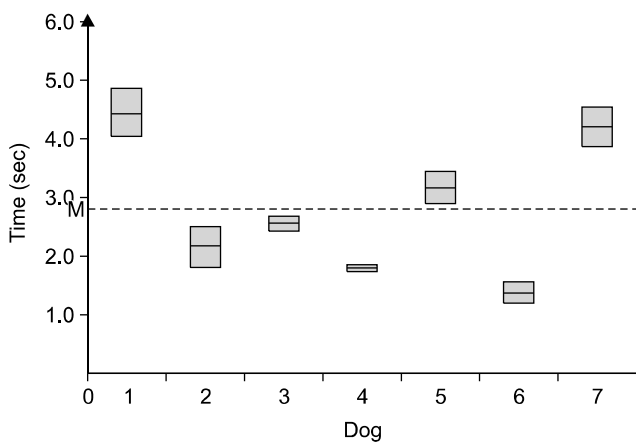
Discussion

In this study, we used color Doppler US to detect urinary flow from the right ureteral orifice in eight healthy beagles. Ureteral jets were detected in all eight dogs. Despite the small number of dogs used, the results of this study illustrate that color Doppler US facilitates the visualization of ureteral jets. Using color Doppler US, the ureteral jet is clearly visualized as a red-colored flow. Thus, the ureteral jet detection rate is high due to the ease of clear visualization via color Doppler US.

When a bolus of urine is being transmitted through the ureter reaches its terminal portion, it is forcefully ejected into the bladder through the VUJ [24,26]. US images of the ureteral jet have been consistently obtained in both humans and dogs [5,10,23,24]. The jet can be detected via gray-scale imaging as a stream or burst of low-intensity echoes emerging from the

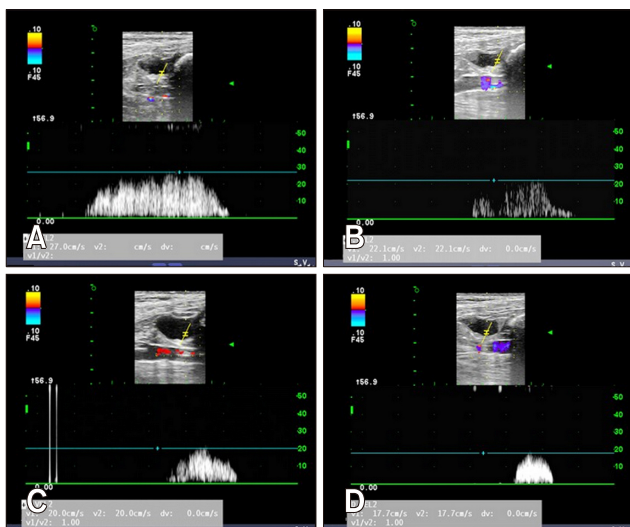**Fig. 7.** Mean ureteral jet duration in each dog and mean duration in all dogs (M).

Fig. 8. Spectral Doppler images of changing jet appearance and duration.
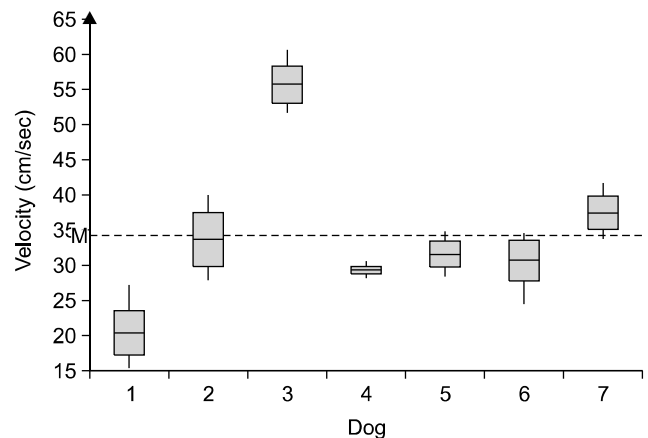

Fig. 9. Mean ureteral jet peak velocity in each dog and mean value in all dogs (M).

ureteral orifice [24,25]. The jet lasts for only a few seconds, but its speed is sufficient to produce a frequency shift, thereby allowing both color and Doppler waveforms to be obtained in real time [25]. The ureteral jet can be further characterized by examining its pulsed Doppler waveform, which has been related to vesicoureteric sphincter function in humans [24-26]. However, this phenomenon is not always detected in humans and dogs; interestingly, it only appears to occur when certain requirements are met. Specifically, a difference in urinary specific gravity between the ureter and bladder, appropriate hydration level, and the bladder filling status have been shown to be required for its appearance [2,10,19,23,34].

Unlike humans, dogs cannot control their fluid intake and urination. However, it is difficult to examine ureteral jets in dogs under natural conditions. Therefore, a specific method is required to measure the ureteral jet consistently. Such a method would allow research into this phenomenon in dogs and could be useful when applied in clinical practice in veterinary medical science. It has been reported that a contrast medium and sterile saline can be injected into the bladder of dogs to detect a constant jet [23]; however, in our experiment, a consistently distinctive ureteral jet flow was detected within 5 min by using only intravenous hydration with 0.9% saline and a diuretic. In the present study, without controlling the difference in urinary specific gravity between the bladder and ureter before the examination, ureteral jets were identified in all eight dogs.

On US and magnetic resonance imaging, the ureteral jet is usually directed either cranially or craniomedially, with or without crossing of the jets [10,11,24]. Other studies have shown that ureteral jets can move in a vertical direction or perpendicular to the dorsal surface of the bladder [3,4,5,15,33,37]. The results we obtained by using color Doppler US in seven dogs are similar to those reported in previous studies of humans.

US has been described as an accurate and noninvasive method for evaluating the renal collecting system, and it is commonly used in cases of suspected renal obstruction [1,6,12,13,17,22,31,35,40]. Although gray-scale US provides important anatomic information, it cannot differentiate between obstructive and non-obstructive dilatation of the renal collecting system [1,12,17,21,38,39]. The use of pulsed and color Doppler US has enabled the evaluation of the function and obstruction of both kidney and ureter [9]. It was previously suggested that the presence of a ureteral jet could be used to exclude complete ureteral obstruction, and the complete absence of a jet is symptomatic of a high-grade obstruction caused by ureteral calculi in humans [3,8,11,14,21,25,36,38,42]. Complete obstruction can be reliably ascertained by the absence of a ureteral jet on the suspected side of the obstruction with extremely high sensitivity and specificity [9]. The present study illustrates that ureteral jets can be consistently visualized in dogs by using a simple technique, suggesting that non-visualization of the ureteral jet could potentially be used as a diagnostic tool to assess obstruction of the ureter in dogs, as in humans.

In the present experiment, ureteral jet observation became more difficult over time, and, in five dogs, the jets disappeared completely during the 40−60 min observation period. In another Doppler US study, a markedly distended bladder was demonstrated in dogs, and therefore, it was not possible to detect ureteral jets or record Doppler signals from the ureteral orifices in those animals. It is assumed that, based on previous reports and our experiments, several factors could have affected the loss of jets in the present study, including a smaller difference in urinary specific gravity between the bladder and ureter, excessive distention of the bladder, and a reduction in the efficacy of the diuretic [2,10,19,23,34]. In particular, when the urinary bladder is filled to a certain degree, it is possible that pressure exerted by the distended bladder on the ureters prevents the jet-like entry of urine into the bladder [10]. Although the urinary specific gravity between the ureter and bladder was not controlled in this study, in order to detect ureteral jets it is necessary to control the size of the bladder, if it is not too distended, as noted in previous US Doppler studies [2,10,19,23,34].

The results of the present study demonstrate the existence of various ureteral jet waveform patterns in dogs, as has been also observed in humans. In humans, six patterns have been identified according to the number of peaks within a particular Doppler waveform: monophasic, biphasic, triphasic, polyphasic, square, and continuous [24-26]. These waveforms have been grouped into three categories: 1) the monophasic form is classified as a simple and immature pattern; 2) the bi-, tri-, and polyphasic patterns are classified as complex and mature patterns; and 3) the square and continuous forms comprise a diuretic pattern, and represent a state of forced diuresis [13,22]. In humans, changes in the waveform pattern of the ultimate ureteral jet are thought to be caused by modification of the jet by an active sphincter mechanism at the human VUJ [24-26]. There are two components in the dual-mode action of the functional sphincter: myogenic (primary or immature) and neurogenic components (secondary or mature). The monophasic jet pattern is the result of contraction caused by the myogenic component of the VUJ, whereas the complex pattern is the result of modulation of the myogenic component of the jet by the neurogenic component in response to distal intra-ureteral pressure [24,25,27]. The subsequent ureteral jet waveform varies depending on whether the neurogenic component is active [24,25,27]. Based on the results of previous studies and those in this study, we postulate that the canine VUJ may act as a functional sphincter with myogenic and neurogenic components, as has been observed in humans.

We found a significant reduction in the incidence of the complex waveform pattern in the period starting 10 min after the initial jet appeared; the period in which the ureteral jet was

identified the most distinctively. Only three patterns (monophasic, continuous, and square waveforms) were observed during this period. In humans, when only the myogenic component is functioning, as can be observed in a small immature subject under general anesthesia, or in certain pathological conditions, the jet pattern reverses to the monophasic pattern [24]. It has already been established that, in humans, continuous or square waveforms represent modified waveforms under the state of forced diuresis. Premature relaxation of the VUJ is most likely to be governed by the neural mechanism observed in forced diuresis [5,15,24,26]. Only three patterns were identified in this period, suggesting that the anesthetic and diuretic could have affected the VUJ mechanism. In dogs undergoing unusual physiological conditions, such as general anesthesia and significant diuresis stress, the VUJ mechanism may be altered, and a modified ureteral jet pattern observed. This study was not designed to identify a particular drug or drugs that would produce this change. However, due to the observed changes in the ureteral jet Doppler waveforms to monophasic, continuous, and square patterns, it is assumed that the anesthetic and diuretic were influential factors. The observation of a pharmacological effect on the VUJ supports the hypothesis of an active VUJ sphincter in dogs, as in humans. Further studies may be necessary to determine the correlation between the function of the VUJ and the change in the ureteral jet pattern, and to evaluate the clinical significance of Doppler US-obtained waveforms in dogs.

In humans, under the condition of forced diuresis, the jet has a higher velocity, duration, and frequency than those observed in the normal physiological state [29]. Doppler waveforms in humans under the state of forced diuresis have also been identified. In the present study, the dogs were administered a diuretic and 0.9% saline intravenously during the examination. Based on the results in human studies and those in our experiment, it can be assumed that the ureteral jet velocity, duration, and frequency values recorded in this study would be higher than those in dogs under a normal physiological state.

It was previously reported that urinary volume in humans can be calculated from mean jet velocity, duration, and frequency and the area of the ureteral orifice [29]. Although the area of the ureteral orifice was not measured in the present study, a temporal decrease in the mean peak velocity, duration, or frequency was clearly demonstrated on the spectral Doppler images in the study's seven dogs. Based on previous studies and our results, urinary volume decreases over time and the parameters measured by pulsed Doppler US could be used to estimate urinary volume in dogs, especially when the insertion of a urethral catheter is difficult.

This study has a few limitations. The relatively small number of dogs included in the study and the absence of values obtained under a normal physiological condition limit the power of the statistical results. In addition, the application of the Doppler imaging technique requires technical expertise and high-quality equipment to obtain high accuracy. However, the jet phenomenon of urine propelled from the ureteral orifice was detected clearly by using color Doppler US. The detection of a consistent ureteral jet can be utilized in the assessment of ureteral abnormalities, such as obstruction and ectopic ureter. Further studies may be warranted to evaluate the clinical relevance of the ureteral jet phenomenon in dogs.

Conflict of Interest

The authors declare no conflict of interests.

References

1. **Akçar N, Özkan IR, Adapınar B, Kaya T.** Doppler sonography in the diagnosis of urinary tract obstruction by stone. J Clin Ultrasound 2004, **32**, 286-293.
2. **Baker SM, Middleton WD.** Color Doppler sonography of ureteral jets in normal volunteers: importance of the relative specific gravity of urine in the ureter and bladder. AJR Am J Roentgenol 1992, **159**, 773-775.
3. **Burge HJ, Middleton WD, McClennan BL, Hildebolt CF.** Ureteral jets in healthy subjects and in patients with unilateral ureteral calculi: comparison with color Doppler US. Radiology 1991, **180**, 437-442.
4. **Catalano O, De Sena G, Nunziata A.** [The color Doppler US evaluation of the ureteral jet in patients with urinary colic]. Radiol Med 1998, **95**, 614-617. Italian.
5. **Cox IH, Erickson SJ, Foley WD, Dewire DM.** Ureteric jets: evaluation of normal flow dynamics with color Doppler sonography. AJR Am J Roentgenol 1992, **158**, 1051-1055.
6. **Curry NS, Gobien RP, Schabel SI.** Minimal-dilatation obstructive nephropathy. Radiology 1982, **143**, 531-534.
7. **Daniel EE, Tomita T, Tsuchida S, Watanabe M.** Sphincters: Normal Function-Changes in Diseases. pp. 295-304, CRC Press, Tokyo, 1992.
8. **Delair SM, Kurzrock EA.** Clinical utility of ureteral jets: disparate opinions. J Endourol 2006, **20**, 111-114.
9. **Deyoe LA, Cronan JJ, Breslaw BH, Ridlen MS.** New techniques of ultrasound and color Doppler in the prospective evaluation of acute renal obstruction. Do they replace the intravenous urogram? Abdom Imaging 1995, **20**, 58-63.
10. **Dubbins PA, Kurtz AB, Darby J, Goldberg BB.** Ureteric jet effect: the echographic appearance of urine entering the bladder. A means of identifying the bladder trigone and assessing ureteral function. Radiology 1981, **140**, 513-515.
11. **Elejalde BR, de Elejalde MM.** Ureteral ejaculation of urine visualized by ultrasound. J Clin Ultrasound 1983, **11**, 475-476.
12. **Erwin BC, Carroll BA, Sommer FG.** Renal colic: the role of ultrasound in initial evaluation. Radiology 1984, **152**, 147-150.
13. **Grisi G, Stacul F, Cuttin R, Rimondini A, Meduri S, Dalla Palma L.** Cost analysis of different protocols for imaging a patient with acute flank pain. Eur Radiol 2000, **10**,

1620-1627.

14. **Jafri SZ, Madrazo BL, Miller JH.** Color Doppler ultrasound of the genitourinary tract. Curr Opin Radiol 1992, **4**, 16-23.

15. **Jequier S, Paltiel H, Lafortune M.** Ureterovesical jets in infants and children: duplex and color Doppler US studies. Radiology 1990, **175**, 349-353.

16. **Jubb KVF, Kennedy PC, Palmer N.** Pathology of Domestic Animals. 3rd ed. Vol. 2. pp. 390-392, Academic Press, San Diego, 1985.

17. **Kamholtz RG, Cronan JJ, Dorfman GS.** Obstruction and the minimally dilated renal collecting system: US evaluation. Radiology 1989, **170**, 51-53.

18. **Koelliker SL, Cronan JJ.** Acute urinary tract obstruction: imaging update. Urol Clin North Am 1997, **24**, 571-582.

19. **Kremer H, Dobrinski W, Mikyska M, Baumgärtner M, Zöllner N.** Ultrasonic *in vivo* and *in vitro* studies on the nature of the ureteral jet phenomenon. Radiology 1982, **142**, 175-177.

20. **Kremkau FW, Gramiak R, Carstensen EL, Shah PM, Kramer DH.** Ultrasonic detection of cavitation at catheter tips. Am J Roentgenol Radium Ther Nucl Med 1970, **110**, 177-183.

21. **Laing FC, Benson CB, DiSalvo DN, Brown DL, Frates MC, Loughlin KR.** Distal ureteral calculi: detection with vaginal US. Radiology 1994, **192**, 545-548.

22. **Laing FC, Jeffrey RB Jr, Wing VW.** Ultrasound versus excretory urography in evaluating acute flank pain. Radiology 1985, **154**, 613-616.

23. **Lamb CR, Gregory SP.** Ultrasonography of the ureterovesicular junction in the dog: a preliminary report. Vet Rec 1994, **134**, 36-38.

24. **Leung VY, Chu WC, Yeung Ck, Metreweli C.** Doppler waveforms of the ureteric jet: an overview and implications for the presence of a functional sphincter at the vesicoureteric junction. Pediatr Radiol 2007, **37**, 417-425.

25. **Leung VYF, Chu WCW.** Functional anatomy of the vesicoureteric junction: implication on the management of VUR/ UTI. In: Nelius T (ed.). Recent Advances in the Field of Urinary Tract Infections. Chapt. 6, InTech, 2013.

26. **Leung VYF, Metreweli C, Yeung CK.** The ureteric jet Doppler waveform as an indicator of vesicoureteric sphincter function in adults and children. An observational study. Ultrasound Med Biol 2002, **28**, 865-872.

27. **Leung VYF, Metreweli C, Yeung CK, Sihoe JDY.** Ureteric jet in the anaesthetised child. Ultrasound Med Biol 2003, **29**, 1237-1240.

28. **Marshall JL, Johnson ND, De Campo MP.** Vesicoureteric reflux in children: prediction with color Doppler imaging. Work in progress. Radiology 1990, **175**, 355-358.

29. **Matsuda T, Saitoh M.** Detection of the urine jet phenomenon using Doppler color flow mapping. Int J Urol 1995, **2**, 232-234.

30. **Meltzer RS, Tickner EG, Sahines TP, Popp RL.** The source of ultrasound contrast effect. J Clin Ultrasound 1980, **8**, 121-127.

31. **Mostbeck GH, Zontsich T, Turetschek K.** Ultrasound of the kidney: obstruction and medical diseases. Eur Radiol 2001, **11**, 1878-1889.

32. **Noordzij JW, Dabhoiwala NF.** A view on the anatomy of the ureterovesical junction. Scand J Urol Nephrol 1993, **27**, 371-380.

33. **Patel U, Kellett MJ.** Ureteric drainage and peristalsis after stenting studied using colour Doppler ultrasound. Br J Urol 1996, **77**, 530-535.

34. **Price CI, Adler RS, Rubin JM.** Ultrasound detection of differences in density: explanation of the ureteric jet phenomenon and implications for new ultrasound applications. Invest Radiol 1989, **24**, 876-883.

35. **Saita H, Matsukawa M, Fukushima H, Ohyama C, Nagata Y.** Ultrasound diagnosis of ureteral stones: its usefulness with subsequent excretory urography. J Urol 1988, **140**, 28-31.

36. **Strehlau J, Winkler P, de la Roche J.** The uretero-vesical jet as a functional diagnostic tool in childhood hydronephrosis. Pediatr Nephrol 1997, **11**, 460-467.

37. **Sweet CS, Silbergleit R, Sanders WP.** MRI demonstration of ureteral jet effect in a patient with a spinal ganglioneuroma. Pediatr Radiol 1995, **25**, 574-575.

38. **Tal Z, Jaffe H, Rosenak D, Nadjari M, Hornstein E.** Ureteric jet examination by color Doppler ultrasound versus IVP for the assessment of ureteric patency following pelvic surgery− a pilot study. Eur J Obstet Gynecol Reprod Biol 1994, **54**, 119-122.

39. **Timor-Tritsch IE, Haratz-Rubinstein N, Monteagudo A, Lerner JP, Murphy KE.** Transvaginal color Doppler sonography of the ureteral jets: a method to detect ureteral patency. Obstet Gynecol 1997, **89**, 113-117.

40. **Van Arsdalen KN, Banner MP, Pollack HM.** Radiographic imaging and urologic decision making in the management of renal and ureteral calculi. Urol Clin North Am 1990, **17**, 171-190.

41. **Wu CC, Yao WJ, Lin F Jr, Hsieh HL, Hwang MH.** Spectral analysis of ureteral jets by color Doppler ultrasonography: a preliminary uretero-dynamic study. J Med Ultrasound 1995, **3**, 64-69.

42. **Yoon DY, Bae SH, Choi CS.** Transrectal ultrasonography of distal ureteral calculi: comparison with intravenous urography. J Ultrasound Med 2000, **19**, 271-275.